

# THE ACCRETION DISK SCALE WARM ABSORBER IN NGC 4051

M. Elvis<sup>1</sup>, Y. Krongold<sup>1,2</sup>, F. Nicastro<sup>1</sup>, N. Brickhouse<sup>1</sup> & L. Binette<sup>2</sup>

1. Harvard-Smithsonian Center for Astrophysics, 60 Garden St., Cambridge MA 02138, USA
2. IA-UNAM, Mexico City, Mexico

## ABSTRACT

The warm absorber (WA) of NGC4051 is found to respond rapidly to the changing continuum in XMM EPIC-pn data, requiring high densities in the WA gas, so restricting the WA location

The two components of the WA in NGC4051 – required by RGS - the ‘low’ and ‘high’ ionization phases, are determined to lie a few light-days from the ionizing continuum source, equivalent to 2200-4400  $R_g$ . The implied mass loss rates are a few percent of the accretion rate. This suggests that AGN winds are not capable of affecting galaxy-AGN co-evolution.

## 1. WARM ABSORBERS

Ionized, or ‘Warm’ Absorbers (WAs) are a common signature of winds in AGNs, seen in both UV and X-rays for  $\sim 50\%$  of AGNs (Crenshaw, Kraemer & George 2003). Depending on the mass outflow rate of these winds they may influence their host galaxies, potentially controlling the ‘co-evolution’ that is required by the M- $\sigma$  relation. While we know the line-of-sight velocity of these winds ( $\sim 500$ -  $\sim 2000$  km s<sup>-1</sup>), their mass flux is uncertain by a factor  $10^6$ , due to our lack of knowledge of where the wind arises, as the two are proportional.

Suggested locations range from the kpc-scale narrow emission line region (Kinkhabwala et al. 2002), to the pc-scale obscuring molecular torus (Krolik & Kriss 2001), to the  $\sim 1000 R_g$  scale of the accretion disk (Elvis 2000, 2004). This ignorance can be lifted by employing non-equilibrium photoionization models to time variable AGNs (Nicastro et al. 1999). Figure 1 illustrates how a step function change in the continuum produces a rapid, though not instantaneous, change in dense gas, and a slow change in low density gas. Early attempts used primitive models of the WA that used only a few bound-free transitions and relatively low signal-to-noise spectra. We now have far more complete WA models including large numbers of bound-bound transitions (Figure 2, Krongold et al.) from extensive databases (APED, Smith, Brickhouse & Liedahl, 2003).

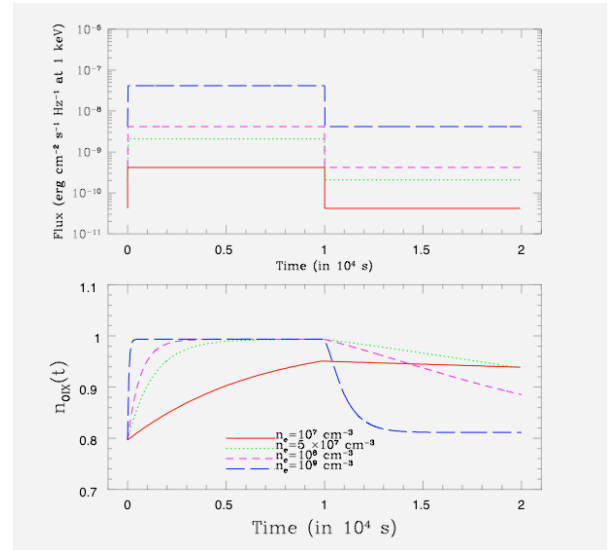


Figure 1: Response of photo ionized gas to a step function change in the ionizing continuum for various densities (Nicastro et al. 1999).

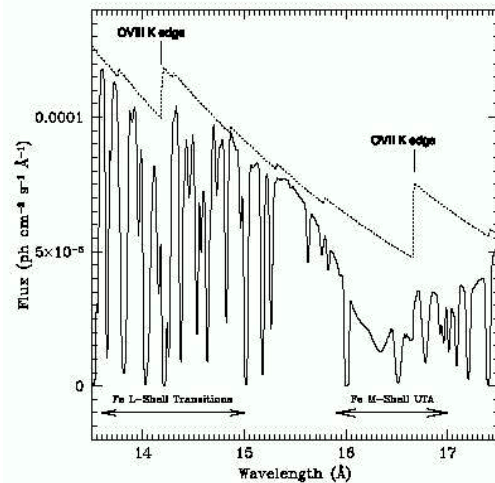


Figure 2: Comparison of full PHASE photoionized absorber model with the component due just to bound-free transitions (Krongold et al. 2003).

## 2. NGC 4051

NGC4051 varies rapidly (<1hour) and with large amplitude (factor 3-10). This makes NGC4051 an excellent test case for determining the density and hence location of a warm absorber (WA), using the timescale on which the WA gas responds to changes in the ionized continuum. As NGC 4051 has a known black hole mass ( $2 \times 10^6 M_\odot$ ) from reverberation mapping (Peterson et al. 2004) we can further restrict the WA location in Schwartzchild radii.

XMM-Newton observed NGC4051 for 117 ksec in 2001 May. We have reanalyzed the archival data for this observation using the PHASE code (Krongold et al. 2003) to determine the WA properties.

## 3. NGC 4051 XMM-NEWTON SPECTRA

The XMM-Newton RGS data in the high state required a two-component WA in order to fit the spectrum. The ionization state of the low and high ionization phases (LIP, HIP) are similar to those of NGC3783 (Krongold et al. 2003) but with smaller column densities.

Using these two components we then fitted the EPIC-pn data for 21 separate intervals along the light curve, chosen to have roughly constant flux during each interval. We found that two components were required for EPIC too, but that the derived ionization parameters,  $U_X$  (Netzer 1996), changed systematically with the continuum flux. Figure 3 shows the light curve, the binned light curve, and the derived values of  $U_X$  for the two components.

## 4. RAPID RESPONSE OF THE WARM ABSORBERS

Clearly the ionization parameters track the ionizing flux close to the way expected for gas in photoionization equilibrium. This can be seen more precisely by noting the squares in the two  $U_X$  plots, which show the values expected for gas keeping precisely to photoionization equilibrium.

This behavior immediately requires a dense and, as the column density is fixed, compact WA. A NELR origin is thus ruled out. Moreover continuous flow models are also ruled out. In these models the WA is a continuous medium extending over a factor of several in radius with gradually decreasing ionization parameter. Such a WA will not respond strongly to changes in the continuum as gas ionized up from state  $i$  to  $i+1$  is compensated for by gas ionized from  $i-1$  to  $i$ . This result has already been found to apply to NGC 3783 (Krongold et al. 2004).

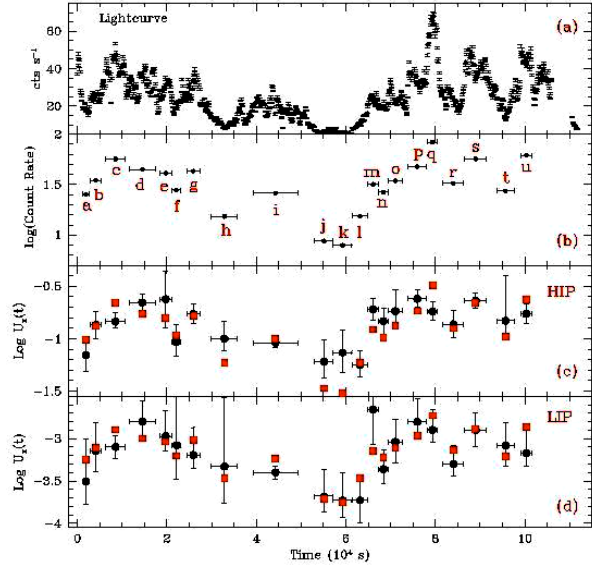


Figure 3: (a) XMM-Newton light curve of NGC4051 and (b) binned in 21 intervals; (c)(d) ionization parameters,  $U_X$  for the high (HIP) and low (LIP) ionization WA required by the RGS. The squares show  $U_X$  for gas in photoionization equilibrium.

We can make more quantitative estimates of the WA gas density for each phase. Figure 4 shows  $U_X$  vs. continuum count rate for the high low ionization phase (LIP) of the WA fits. As one would expect from the light curves, the two are well correlated. The normalization of these plots determines the WA density-radius-squared product,  $n_e R^2$ , robustly.

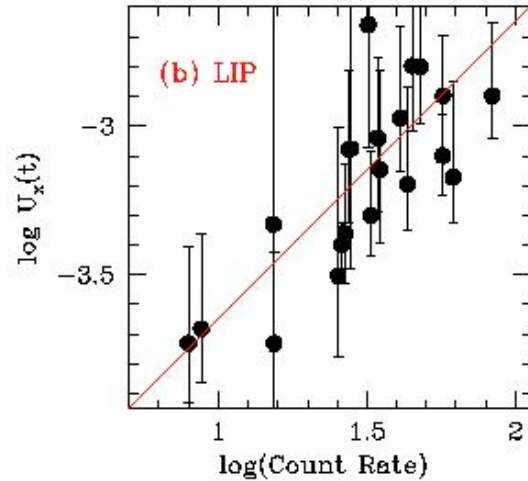


Figure 4:  $U_X$  versus continuum count rate for the low ionization WA phase (LIP).

For the LIP there is no departure from ionization equilibrium even at extreme fluxes and down to the shortest timescale of variability of 3 ksec. This implies  $n_e(LIP) > 8.1 \times 10^7 \text{ cm}^{-3}$ . But  $n_e R^2 = 6.6 \times 10^{39} \text{ cm}^{-1}$ . So

we derive an upper limit on the distance of the LIP from the ionizing continuum of  $r(LIP) < 8.9 \times 10^{15}$  cm, which is  $< 0.0029$  pc, or  $< 3.5$  light-days.

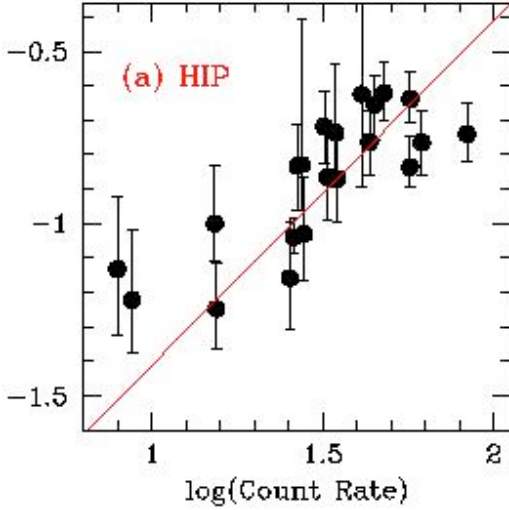


Figure 5: UX versus continuum count rate for the low ionization WA phase (LIP).

The high ionization phase (HIP) presents a different and more constraining picture (figure 5). Here the HIP is out of photoionization equilibrium at the highest and lowest continuum fluxes, but in equilibrium at intermediate fluxes. In this observation we are just resolving the ionization and recombination times of the HIP. It is reasonable that it is the HIP which has a resolved response time: if the HIP and LIP are co-spatial then the higher ionization phase will have lower density and so should be slower to respond to continuum changes.

Quantitatively we find that the HIP density is tightly constrained to about a factor 2:  $n_e(HIP) = (0.6-2.1) \times 10^7 \text{ cm}^{-3}$ . This translates into a radius,  $r(HIP) = (1.3-2.6) \times 10^{15}$  cm, which is (0.5-1.0) light-days.

The first thing to note is that the LIP and HIP are consistent with being at the same radius and so could be co-spatial as assumed in previous studies. Moreover, as PHASE also determines a temperature, we can determine the HIP and LIP pressures independent of assuming co-spatiality.

Again the pressures turn out to be consistent with pressure equilibrium between the two phases:  $P(HIP) = (2.9-10.5) \times 10^{12} \text{ K cm}^{-1}$ , while  $P(LIP) > 2.4 \times 10^{12} \text{ K cm}^{-1}$ .

The thickness of the two WA phases (assuming each is continuous) can also be found as  $\Delta R = 1.23 N_H / n_e$ .  $\Delta R(LIP) < 9 \times 10^{12} \text{ cm}$ ;  $\Delta R(HIP) = (1.9-7.2) \times 10^{14} \text{ cm}$ . This yields surprisingly thin radial extents compared with their radii:  $(\Delta R/R)_{HIP} = 0.1-0.2$ ,  $(\Delta R/R)_{LIP} < 10^{-3}$ .

The particularly thin LIP  $\Delta R/R$  suggests that this phase is either a boundary layer around the HIP, or is mixed within the HIP in pressure equilibrium – which may be preferred given the consistency with pressure balance of the two phases.

## 5. THE LOCATION OF THE AGN WIND

We already ruled out the kpc-scale NELR as the location of the AGN wind seen in the WA. These quantitative distance determinations allow us to go much further (figure 6).

For a source with the continuum luminosity of NGC 4051 the minimum dust sublimation radius is 12-170 days (Barvainis 1987). As both WA components lie within 3.5 light-days this rules out the inner edge of the dusty molecular torus (Krolik & Kriss 2001) of unification models (Urry & Padovani 1995 as the source of the AGN wind, at least in this AGN. Reverberation mapping also locates the H $\beta$  emitting broad emission line region (BELR) outside the WA location, at 5.9 light-days (Peterson et al. 2000).

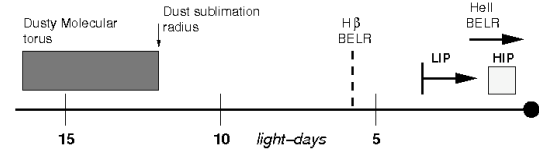


Figure 6: Location of nuclear features in NGC4051 on a light-days scale.

Zooming in closer to the AGN (figure 7), we recall that the BELR in AGNs is stratified, with higher ionization lines being closer to the nucleus (Clavel et al. 1991). In NGC4051 the high ionization line HeII (4686A) comes from a region  $< 2$  light-days from the continuum source. The high ionization BELR is thus consistent with the location of the WA wind. Interestingly the HeII emission line has a blue asymmetry of  $\sim 400 \text{ km s}^{-1}$ , suggestive of an outflow at a velocity similar to that of the WA wind (600–2400  $\text{km s}^{-1}$ , Collinge et al. 2001).

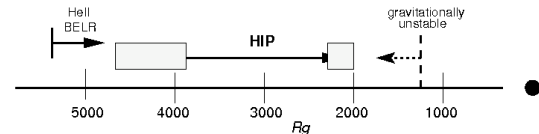


Figure 7: Location of features in NGC4051 on a Schwartzchild radii,  $R_g$ , scale.

Because NGC4051 has a measured black hole mass of  $(1.9 \pm 0.78) \times 10^6 M_\odot$  (Peterson et al. 2004), we can convert the WA HIP location into Schwartzchild radii: 2200 – 4400  $R_g$ . This location suggests a connection with the accretion disk gravitational instability radius

which, is  $r_{grav} = 1330(\kappa/\kappa_{es})^{2/3}r_g$  (Goodman 2003), for nominal standard parameters. However as the disk opacity,  $\kappa$ , could well be 1000 times the electron scattering opacity,  $\kappa_{es}$ , this may be merely a coincidence.

## 6. GEOMETRY OF THE AGN WIND

The thinness of the wind might suggest that AGN winds consist of a series of repetitive impulsive outbursts. However, given the thinness of the WA-HIP these would have a duty cycle of no more than 10-20%. However WAs are seen in at least 50% of all AGNs, leading to an apparent paradox.

This problem was encountered before in the puzzle of the 20-year persistence of the CIV narrow absorption line (NAL) in NGC5548 by Mathur, Elvis & Wilkes (1995). These authors suggested that the solution was to discard spherical symmetry. They proposed instead that the outflow velocity we see is just a component of the true space velocity of the wind, which is moving primarily *across* our line of sight. Higher resolution observations of the WA wind in the UV (Arav, Korista & deKool 2002) make a strong case for a transverse flow dominating the AGN WA wind. The simplest geometry is then a bi-conical flow (Elvis 2000).

## 7. MASS LOSS RATE IN THE AGN WIND

With the assumption of a conical flow, we can derive a mass loss rate in the WA wind:

$$M_{out} = 0.8\pi m_p N_H v_r R f(\theta) \sim (4-9) \times 10^{-5} M_\odot \text{ yr}^{-1}$$

As NGC4051 has an accretion rate of  $0.05M_{\text{Edd}}$  (Peterson et al. 2000), this outflow rate corresponds to 2% - 5% of  $M_{\text{acc}}$ . [The function  $f(\theta)$  has a value close to unity except for extreme viewing angles.]

This contrasts sharply with the far larger mass loss rates obtained by previous studies which assumed  $R$  of order parsecs.

We note that if viewed along the flow direction the wind in NGC4051 would have a 10 times larger column density ( $Rn_e \sim 5 \times 10^{22} \text{ cm}^{-2}$ ), and a larger velocity by up to factor 10. The NGC4051 wind would then approach the observed properties of a BAL (Broad Absorption Line) quasar wind (Elvis 2000). The uncertainty in the correct terminal velocity means that we have only a lower limit to the total kinetic power of the wind, which is only  $\sim 2.5 \times 10^{37} \text{ erg s}^{-1}$ . Assuming the wind achieves escape velocity (else it is not a wind) from  $2200R_g$ , we get a  $\sim 100$  times larger kinetic power.

## 8. IMPLICATIONS & CAVEATS

With a mass loss rate of 2%-5%  $M_{\text{acc}}$  integrating over a somewhat generous  $10^8 \text{ yr}$  lifetime for an AGN outburst, gives a total ejected mass of  $(0.4-2) \times 10^4 M_\odot$  and the total energy carried by the wind is  $10^{45}-10^{47} \text{ erg}$ .

If all AGN winds arise at the same value of  $R_g$  then the mass loss rate scales with the black hole mass and, for more typical masses of  $10^8-10^9 M_\odot$ , the total ejected mass per quasar is  $10^6-10^7 M_\odot$ . This is comparable to that ejected by a ULIRG (Bland-Hawthorn 2005).

Similarly the total energy deposited by a quasar wind would be  $10^{47}-10^{49} \text{ erg}$ .

This observation fits 5 separate predictions of the ‘funnel wind’ model of Elvis (2000, 2004). The AGN wind in NGC4051 is found to be:

1. on the accretion disk scale;
2. consistent with the location of the high ionization BELR;
3. consistent with pressure balanced phases;
4. non-spherical and consistent with conical;
5. similar to a BAL quasar if viewed in the wind flow direction.

This gives us some confidence in this model.

NGC4051 is only one AGN, and has somewhat unusual properties, which must lead to caution in accepting this result as typical of the whole AGN population:

- Low black hole mass;
- Unusually distant BELR (NGC4051 is a narrow line Seyfert 1);
- Unusually weak wind? (as judged from eigenvector 1).

The EPIC-pn is not sensitive to higher ionization WA phase, e.g. one shown only by Fe-K absorption. Some quasars appear to have fast winds with high  $N_H$  in this highest WA state (Pounds et al. 2003). In this sense our wind mass loss rate and kinetic luminosity values are lower limits.

## 9. CONCLUSIONS

We have used the non-equilibrium photoionization technique of Nicastro et al. (1999) to make the first measurement of the density and location of an AGN warm absorber wind. We demonstrate that:

- AGN WA winds arise on accretion disk scales;
- NELR or molecular torus origins are ruled out;
- Continuous flow models are ruled out;

- A spherical geometry is unlikely, while a bi-cone is favored
- Multiple predictions of the Elvis (2000) model are upheld;
- The mass loss rate is small, a few percent of  $M_{\text{acc}}$ .
- The kinetic power may be small, but depends on the unobserved terminal velocity of the wind.

We can test the spherical flow model by re-observing NGC4051 with XMM-Newton. As the line-of-sight velocity is close to 1 light-day/year, repeating the same experiment will give a clear distinction between a transverse flow ( $R \sim 1$  light-day, always) and a radial flow ( $R \sim 4$  light-days after 3 years).

We also need to establish wind locations, densities, mass loss rates and kinetic powers for more typical AGNs. The less dramatic and reliable variability of other AGNs will require long monitoring campaigns. Without this investment however, the extrapolation to the total mass and energy available from AGN winds to affect galaxy evolution will remain too uncertain to test co-evolution models.

NASA grant GO4-5126X (*Chandra*) and grant UNAM-PAPIIT IN118905 partially supported this work.

## REFERENCES

- Arav N., Korista K., & deKool M., 2002 ApJ, 566, 699  
 Barvainis R., 1987, ApJ, 320, 537  
 Bland-Hawthorn J., 2005, AnnRevA&A, 43, 769  
 Clavel, J., 1991, MNRAS, 246, 668  
 Collinge M.J., et al. 2001, ApJ, 557, 2  
 Crenshaw D.M., Kraemer S.B., & George I.M., 2003, Ann.Rev.A&A, 41, 117  
 Elvis M., 2000, ApJ, 545, 63  
 Elvis M., 2004, ASP Conf. Proc. 311, 109  
 Goodman, J., 2003, MNRAS, 339, 937  
 Kinkhabwala et al., 2002, ApJ, 575, 732  
 Krolik J.H., & Kriss G.A., 2001, 447, 512  
 Krongold Y., et al., 2003, ApJ, 597, 832  
 Krongold Y., et al., 2004, ApJ, 622, 842  
 Mathur S., Elvis M., & Wilkes B.J., 1995, ApJ, 452, 230  
 Netzer H., 1996, ApJ, 473, 781  
 Peterson B.M., et al., 2000, ApJ, 542, 161  
 Peterson B.M., et al., 2004, ApJ, 613, 682  
 Urry M., & Padovani P., 1995, PASP, 107, 803

